
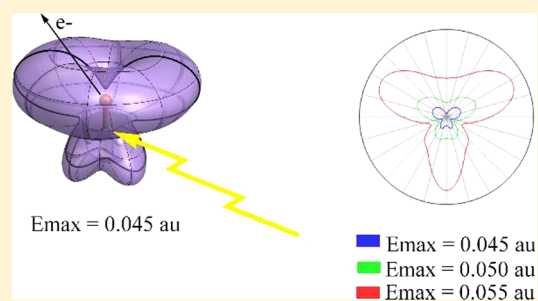


Angular Dependence of Strong Field Ionization of CH₃X (X = F, Cl, Br, or I) Using Time-Dependent Configuration Interaction with an Absorbing Potential

Paul Hoerner and H. Bernhard Schlegel*

Department of Chemistry, Wayne State University, Detroit, Michigan 48202, United States

ABSTRACT: Methyl halides have been used to test basis set effects on simulations of strong field ionization using time dependent configuration interaction with an absorbing potential. Standard atom centered basis sets need to be augmented by several sets of diffuse functions on each atom so that the wave function in the strong field can interact with the absorbing potential used to model ionization. An absorbing basis of 3 s functions, 2 p functions, 3 d functions, and 1 f function is sufficient for CH₃F. Large absorbing basis sets with 4 s functions, 3 or 4 p functions, 4 or 5 d functions, and 2 f functions are recommended for the heavier halogens. The simulations used static fields in the 0.035–0.07 au range to explore the angular dependence of ionization of methyl halides. CH₃F ionizes mainly from the methyl group; CH₃Cl and CH₃Br show ionization from both the methyl group and the halogen, and CH₃I ionizes almost exclusively from the p_π orbitals of the iodine.



INTRODUCTION

Strong field ionization and fragmentation of methyl halides CH₃X (X = F, Cl, Br, or I) have been the subject of several recent studies.^{1–19} Angle- and momentum-resolved measurements of dissociative ionization and Coulomb explosion reveal an asymmetry that changes as the halogen is varied.² With short, intense two color pulses (38 fs, ca. 10¹⁴ W cm⁻², 800 and 400 nm), ionization of CH₃F is favored from the CH₃ group (i.e., when the field points from CH₃ to F), but ionization of the other methyl halides is favored from the halogen side (i.e., when the field points from X to CH₃). This is in accord with the shapes of the highest occupied molecular orbitals (HOMOs). The asymmetry can be modeled by weak field asymptotic theory (WFAT),^{20–23} provided that the Stark effect from methyl halide dipole moment is taken into account.²

In previous studies, we examined the angular dependence of strong field ionization of several small molecules, first and second row hydrides, and various molecules with multiple bonds.^{24–29} We used time dependent configuration interaction with a complex absorbing potential (TDCIS-CAP) to simulate ionization by short, intense 800 nm pulses. The angle dependence can be readily interpreted in terms of the highest occupied molecular orbitals. Depending on the intensity and the polarization direction of the laser pulse, lower lying orbitals can also contribute. Our simulations of strong field ionization use molecular electronic structure methods to calculate the excitation energies and transition dipoles. For the wave functions to interact with the absorbing boundary, the standard atom centered basis functions need to be augmented by several sets of diffuse functions. A suitable set of diffuse basis functions was constructed and tested for TDCIS-CAP calculations of strong field ionization of hydrogen atom and small molecules containing first row atoms.^{24,25} These

absorbing basis sets were also tested and utilized by Lopata and coworkers³⁰ in real-time time-dependent density functional theory (rt-TD-DFT) calculations of the ionization rates of H atoms, N₂, and iodoacetylene (HCCI). The purpose of this short paper is to develop corresponding absorbing basis sets that are suitable for higher rows of the periodic table and test them by simulating the angular dependence of strong field ionization of methyl halides.

METHODS

Ionization in a strong field was simulated by propagating the electronic wave function with the time-dependent Schrödinger equation,

$$i\frac{\partial}{\partial t}\Psi_{\text{el}}(t) = [\hat{H}_{\text{el}} - \hat{\mu}\vec{E}(t) - i\hat{V}^{\text{absorb}}]\Psi_{\text{el}}(t) \quad (1)$$

$$\Psi_{\text{el}}(t) = \sum_{i=0} C_i(t)|\Psi_i\rangle \quad (2)$$

where \hat{H}_{el} is the field-free electronic Hamiltonian. The time-dependent wave function is expanded in the basis of the Hartree–Fock ground state and all singly excited states of the field-free, time-independent Hamiltonian. Interactions between wave function and field are treated in the semiclassical dipole approximation, where $\hat{\mu}$ is the dipole operator and \vec{E} is the electric field. A complex absorbing potential (CAP), $-i\hat{V}^{\text{absorb}}$, is used to model ionization, as described in our previous papers.^{24–29} The absorbing potential is constructed from a set of overlapping spherical potentials centered around each atom, as shown

Received: June 21, 2017

Published: July 17, 2017

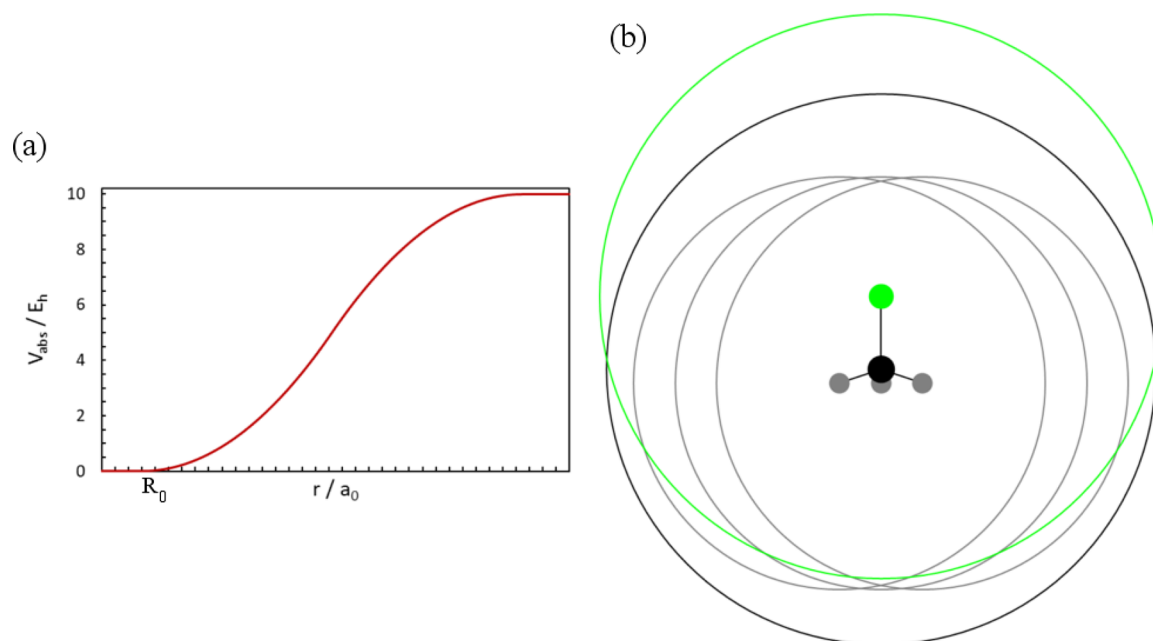


Figure 1. (a) The radial part of the spherical absorbing potential for an atom starts at R_0 and rises gradually to a constant value of 10 hartree. (b) The molecular absorbing potential for CH_3Cl showing the starting radii for each atom. The starting point of the molecular absorbing potential is equal to the maximum of the starting radii for the atomic potentials.

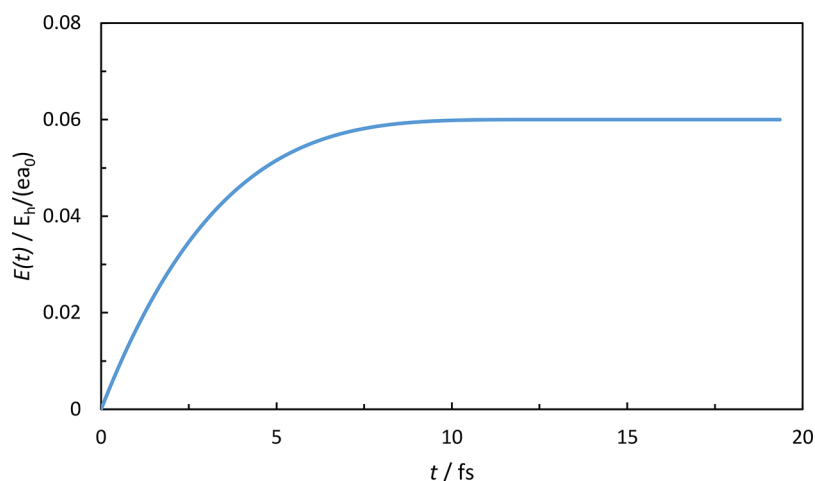


Figure 2. Electric field used in the simulations rises from zero and gradually turns over to a constant value (see eq 3).

Table 1. Exponents for the Uncontracted Gaussian Functions in the Absorbing Basis

type	basis A	basis B	basis C
s	0.0256	0.0256	0.0256
	0.0128	0.0128	0.0128
	0.0064	0.0064	0.0064
p		0.0032	0.0032
	0.0256	0.0256	0.0256
	0.0128	0.0128	0.0128
		0.0064	0.0064
d			0.0032
	0.0512	0.0512	0.0512
	0.0256	0.0256	0.0256
	0.0128	0.0128	0.0128
		0.0064	0.0064
f			0.0032
	0.0256	0.0256	0.0256
		0.0128	0.0128

in Figure 1. The total absorbing potential for the molecule is equal to the minimum of the values of the atomic absorbing potentials. Each spherical potential begins at 3.5 times the van der Waals radius of each element ($R_{\text{H}} = 9.544$ bohr, $R_{\text{C}} = 12.735$ bohr, $R_{\text{F}} = 11.125$ bohr, $R_{\text{Cl}} = 13.052$, $R_{\text{Br}} = 13.853$ bohr, $R_{\text{I}} = 14.882$ bohr); it rises quadratically to 5 hartree at approximately $R + 14$ bohr and turns over quadratically to 10 hartree at approximately $R + 28$ bohr. The CAP is nearly spherical for CH_3X (Figure 1). To model ionization by a static field using a time-dependent approach, the electric field is ramped up slowly and gradually turns over to a constant value so as not to cause any nonadiabatic excitations. The electric field shown in Figure 2 is given by

$$E(t) = E_{\text{max}} \left(1 - \left(1 - \frac{3}{2} \frac{t}{t_{\text{max}}} \right)^4 \right) \text{ for } 0 \leq t \leq \frac{2}{3} t_{\text{max}}$$

$$E(t) = E_{\text{max}} \text{ for } t \geq \frac{2}{3} t_{\text{max}} \quad (3)$$

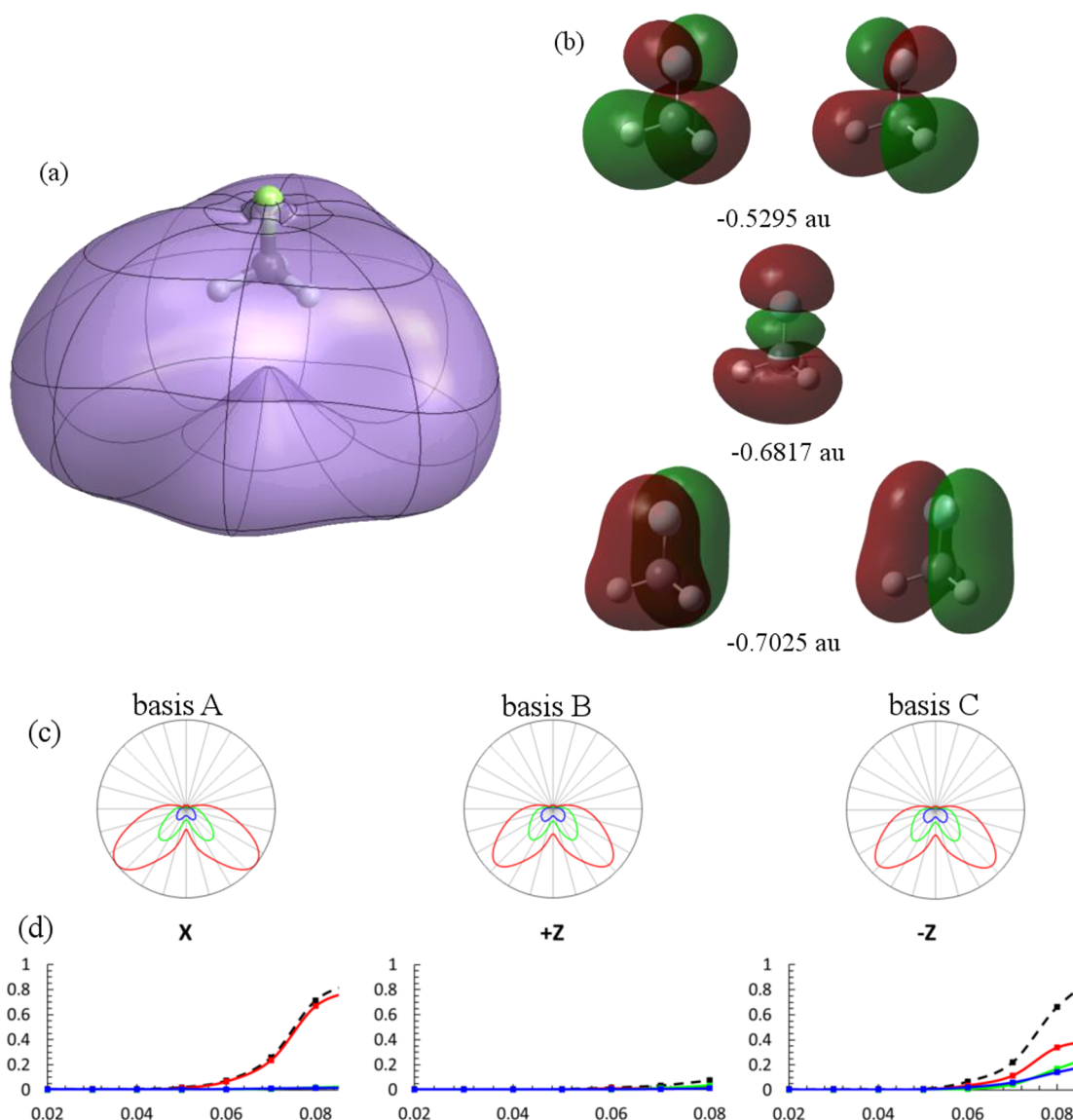


Figure 3. (a) Angular dependence of the ionization rate for CH₃F for a maximum field strength of 0.06 au. (b) Highest occupied molecular orbitals: degenerate π HOMO, σ HOMO-1, and degenerate π HOMO-2. (c) Angle dependence of the ionization rate in the plane containing the C–F bond for basis A, B, and C for field strengths of 0.060 au (blue), 0.065 au (green), and 0.070 au (red). (d) Ionization rate (dashed) and contributions from degenerate π HOMO (red), σ HOMO-1 (green), and degenerate π HOMO-2 (blue) in the +X, +Z, and –Z directions as a function of field strength.

where E_{\max} is the maximum field strength and $t_{\max} = 800$ au = 19.35 fs is the total propagation time. Trotter factorization of the exponential of the Hamiltonian is used to propagate the time-dependent wave function:

$$\begin{aligned} \Psi(t + \Delta t) &= \exp(-i\hat{H}\Delta t)\Psi(t) \\ C(t + \Delta t) &= \exp(-i\mathbf{H}_{el}\Delta t/2)\exp(-\mathbf{V}^{\text{absorb}}\Delta t/2) \\ &\quad \mathbf{W}^T \exp(iE(t + \Delta t/2)\mathbf{d}\Delta t)\mathbf{W} \\ &\quad \exp(-\mathbf{V}^{\text{absorb}}\Delta t/2)\exp(-i\mathbf{H}_{el}\Delta t/2)\mathbf{C}(t) \end{aligned} \quad (4)$$

where $\mathbf{W}\mathbf{D}\mathbf{W}^T = \mathbf{d}$ are the eigenvalues and eigenvectors of the transition dipole matrix \mathbf{D} in the field direction. \mathbf{W} , \mathbf{d} , $\exp(-i\mathbf{H}_{el}\Delta t/2)$, and $\exp(-i\mathbf{V}^{\text{absorb}}\Delta t/2)$ need to be calculated only once because they are time independent. A time step of $\Delta t = 0.05$ au (1.2 as) was used. Reducing the time step by a factor of 2 changed the norm at the end of the propagation by less than 0.01%.

The integrals needed for the TDCIS-CAP simulations were calculated using a modified version of the Gaussian software package.³¹ The Dunning aug-cc-pVTZ basis set^{32–34} was augmented with a set of additional diffused functions (absorbing basis, described below) for adequate interaction with the CAP. The TDCIS simulations were carried out with an external Fortran90 code. Varying the direction of field results in a three-dimensional surface that can be interpreted as the angle-dependent ionization rate. The spherical angles θ and ϕ were changed in steps of 30° for a total of 62 points for each E_{\max} . To obtain smooth surfaces for plotting, ionization yields were fitted to polynomials in $\cos(\theta)^n$, $\cos(m\phi)$, and $\cos(\theta)^n \sin(m\phi)$, $n = 0–7$, $m = 0–6$. Orbital contributions to the ionization are obtained from Mulliken population analysis of the normalized one electron density of the absorbed wave function, $\hat{\mathbf{V}}^{\text{absorb}}\psi_{el}(t)$.

RESULTS AND DISCUSSION

For simulations of strong field ionization with the TDCIS-CAP approach, standard basis sets need to be augmented with

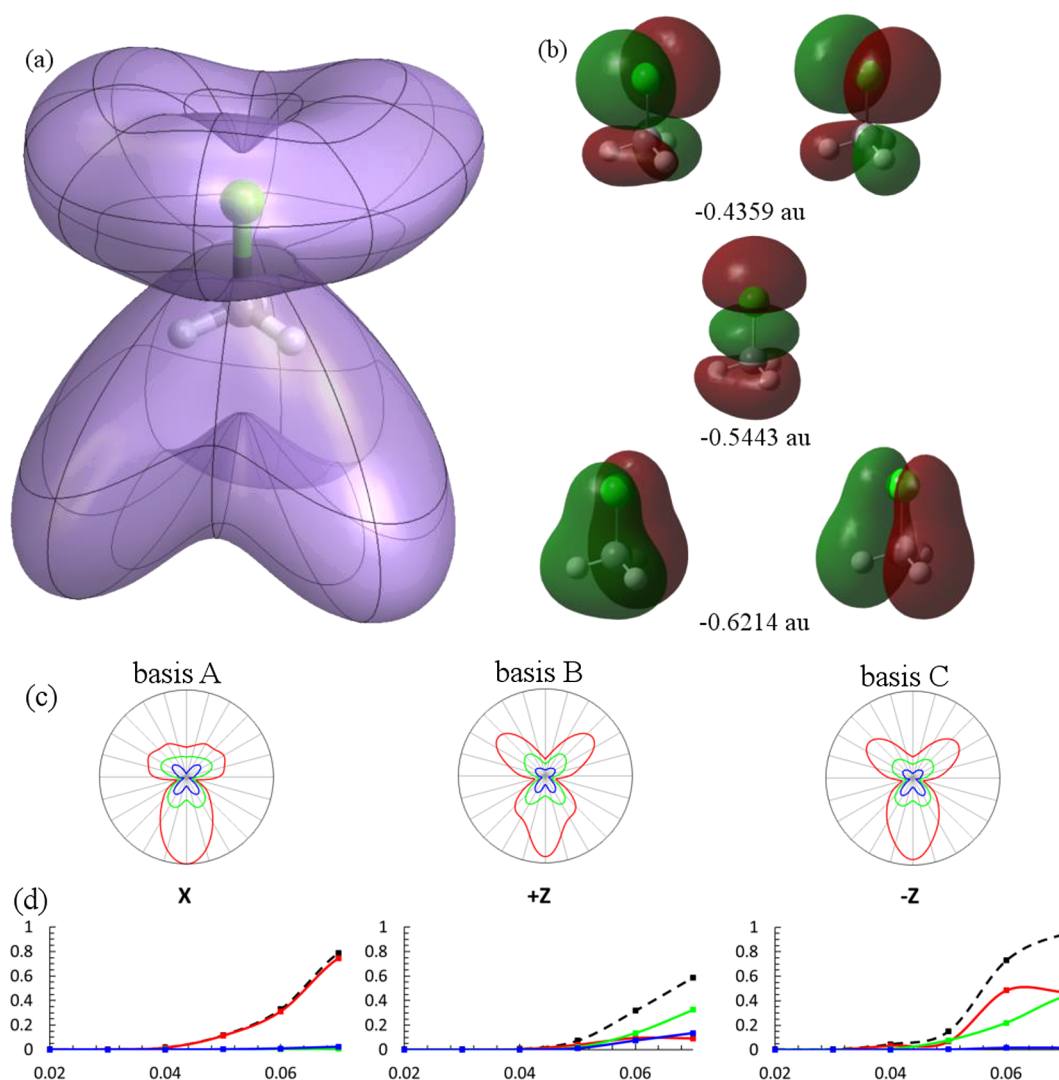


Figure 4. (a) Angular dependence of the ionization rate for CH_3Cl for a maximum field strength of 0.05 au. (b) Highest occupied molecular orbitals: degenerate π HOMO, σ HOMO-1, and degenerate π HOMO-2. (c) Angle dependence of the ionization rate in the plane containing the C–Cl bond for basis A, B, and C for field strengths of 0.050 au (blue), 0.055 au (green), and 0.060 au (red). (d) Ionization rate (dashed) and contributions from degenerate π HOMO (red), σ HOMO-1 (green), and degenerate π HOMO-2 (blue) in the +X, +Z, and –Z directions as a function of field strength.

several sets of diffuse functions to describe the electron as it is propagated from the valence region over the Coulomb barrier toward the absorbing boundary. In previous work, we developed an absorbing basis and tested it on various small molecules, first row hydrides, and molecules containing multiple bonds.^{24–29} As the halogen in CH_3X is changed from $\text{X} = \text{F}$ to I , the electrons in the frontier orbitals are more easily ionized, and a larger absorbing basis may be needed in the ionization simulations. Table 1 lists the exponents of the diffuse uncontracted Gaussian functions that we used for first row systems (basis A) along with two larger basis sets with more diffuse functions (basis B and basis C). These basis sets use spherical harmonic angular factors (i.e., 5 d-type and 7 f-type functions) with exponents that decrease by a factor of 2 for each step. The selection of basis functions needs to be a compromise between small enough exponents to overlap significantly with the absorbing boundary and high enough angular momentum to describe the distortions of the electron density by the field, but not so many functions as to make the simulations impractical. The number of singly excited states

ranged from 1877 for CH_3F with basis A to 4141 for CH_3I with basis C. Such large basis sets can cause SCF convergence problems, and we had to adjust the parameters used for efficient calculations with regular basis sets. In particular, the two electron integrals had to be calculated to an accuracy of 10^{-12} , and variable accuracy and incremental updating of the Fock matrix had to be turned off.

In previous studies, we used an oscillating field with a cosine squared envelope to simulate ionization by an 800 nm laser pulse. However, the total ionization yield for such a laser pulse cannot be used to determine whether ionization of CH_3X occurs primarily from the halogen or the methyl group. Because the electric field oscillates between positive and negative multiple times during the pulse, the total ionization yield with the initial polarization direction parallel to the C–X bond is the same as with the initial direction antiparallel. The effect of directionality of the strong field on ionization rates can be seen more clearly in the simulations if a static field is used instead of an oscillating field. The field in the time-dependent simulation has to be turned on sufficiently slowly to avoid

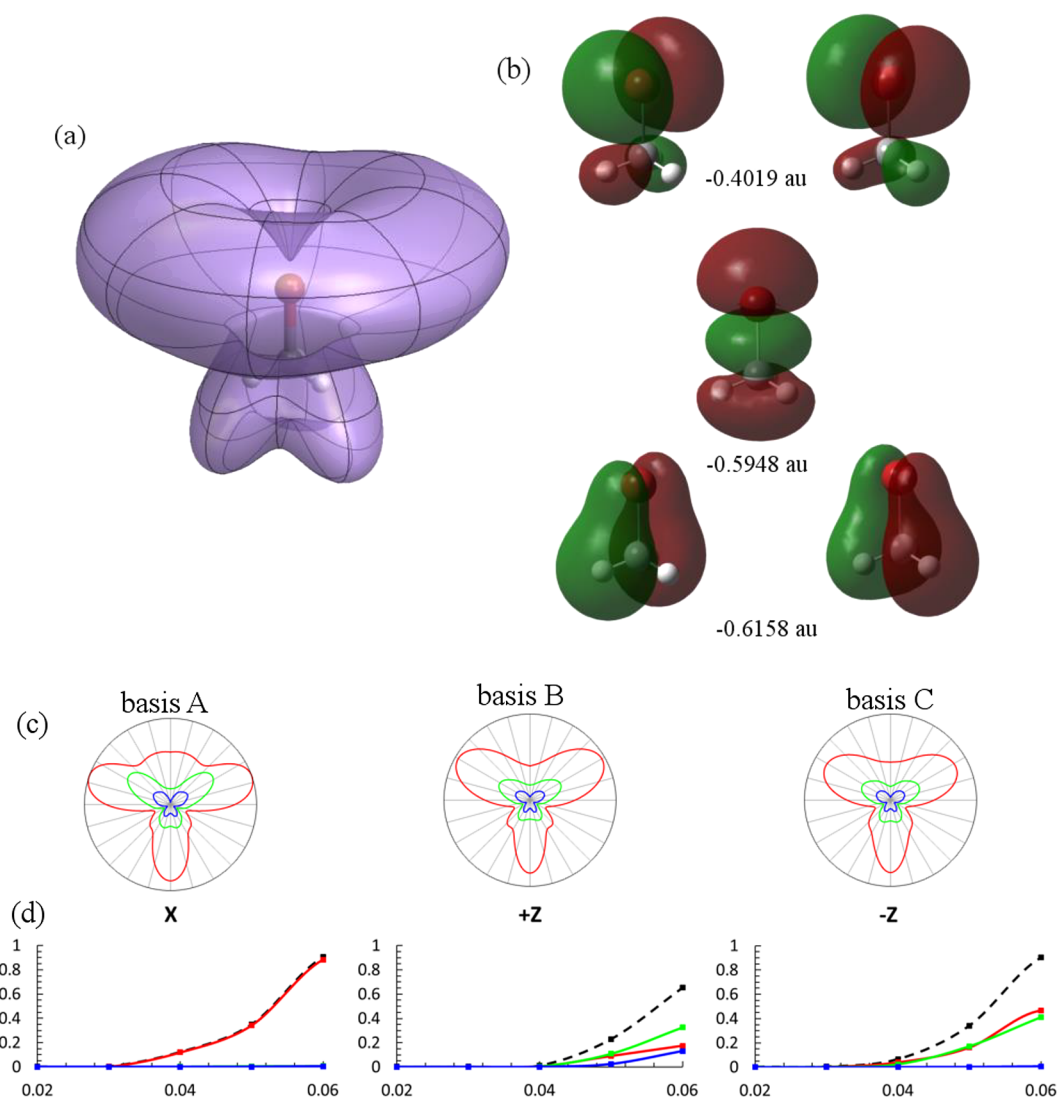


Figure 5. (a) Angular dependence of the ionization rate for CH_3Br for a maximum field strength of 0.045 au. (b) Highest occupied molecular orbitals: degenerate π HOMO, σ HOMO-1, and degenerate π HOMO-2. (c) Angle dependence of the ionization rate in the plane containing the C–Br bond for basis A, B, and C for field strengths of 0.055 au (blue), 0.050 au (green), and 0.055 au (red). (d) Ionization rate (dashed) and contributions from degenerate π HOMO (red), σ HOMO-1 (green), and degenerate π HOMO-2 (blue) in the +X, +Z, and $-Z$ directions as a function of field strength.

nonadiabatic excitation and the field strength had to be low enough to avoid saturation (i.e., $|\Psi(t)|^2$ should not get much below 0.5).

Figure 3a shows the angular dependence of the ionization rate for CH_3F . The magnitude of the rate is plotted radially, and the direction is given by the negative of the electric field vector, i.e. the direction that the electron is accelerated by the electric field. Ionization of CH_3F is dominated by the methyl group. This can be understood qualitatively in terms of the molecular orbitals (Figure 3b). The degenerate HOMO are antibonding combinations of the fluorine π -type lone pairs and the methyl group π -type C–H bonding orbitals. Because the electronegativity of the methyl group is less than the electronegativity of the fluorine, these orbitals have a larger contribution from the methyl group. The resulting orbital shape is in accord with the higher ionization rate from the methyl side of the molecule. Figure 3c illustrates effect of the absorbing basis on the angle dependence of the ionization rates in the plane that contains the C–F bond and is perpendicular to the HCF plane. The

shapes of the ionization rates are essentially the same for the three basis sets. This suggests that basis A is sufficient for molecules containing second period elements at these field strengths. Figure 3d shows the orbital contributions to the ionization rates. For the X direction (and similarly for Y), ionization is almost exclusively from the π HOMOs. In the Z direction, ionization is much greater from the methyl group ($-Z$ direction) than from the fluorine (+Z direction). In both cases the HOMOs are still the largest contributor (accounting for about half of the rate), but there are also sizable contributions from σ HOMO-1 and π HOMO-2.

For CH_3Cl (Figure 4a), the ionization rates from the CH_3 and Cl sides of the molecule are more nearly equal. The π HOMOs have a somewhat larger component of the chlorine p_π orbitals, and this is clearly seen in the 3D shape of the ionization rate. In the 2D plots (Figure 4c), the shapes of the ionization rate change significantly going from basis A to C, indicating that the larger absorbing basis is needed in the ionization simulation. Figure 4d shows that the ionization in the

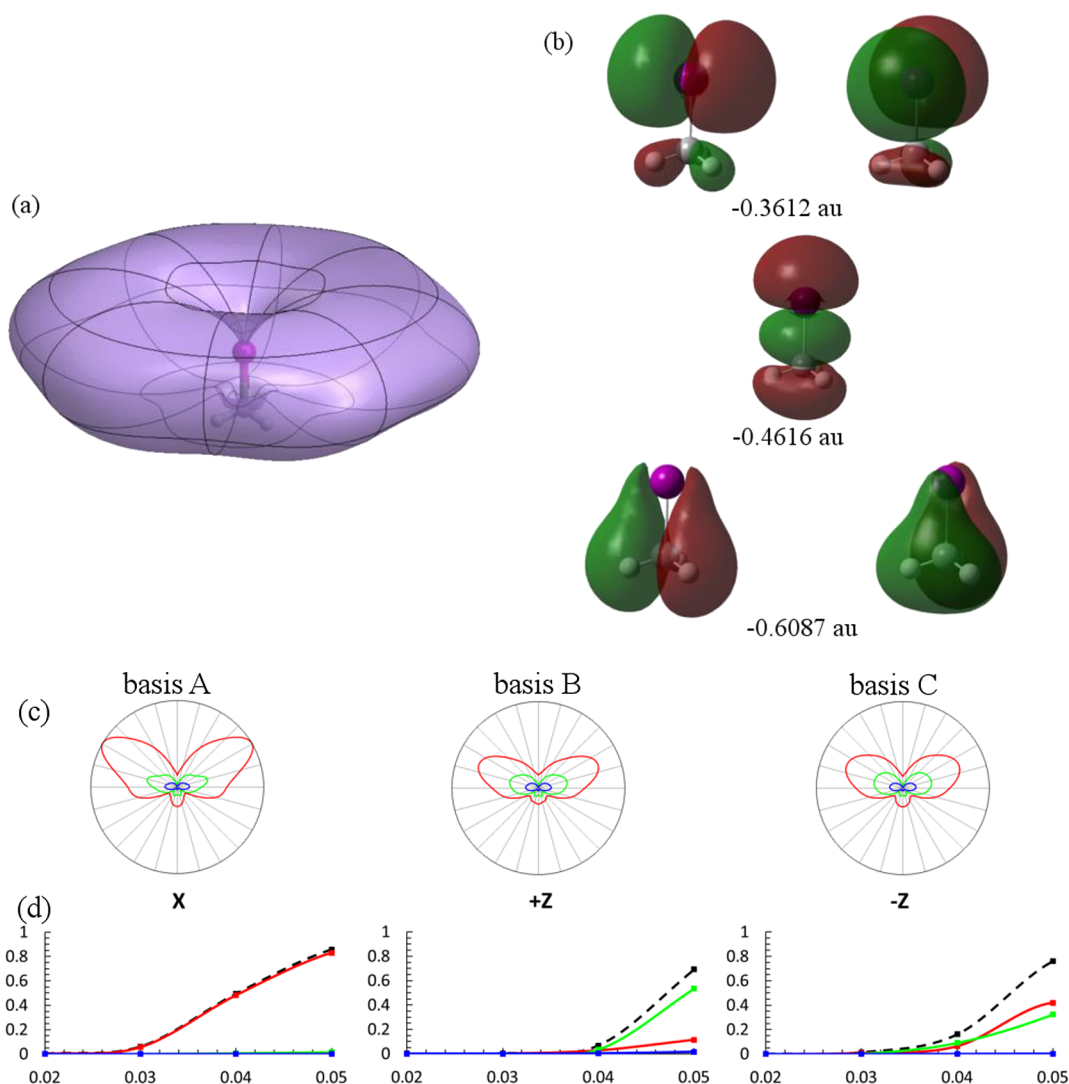


Figure 6. (a) Angular dependence of the ionization rate for CH₃I for a maximum field strength of 0.035 au. (b) Highest occupied molecular orbitals: degenerate π HOMO, σ HOMO-1, and degenerate π HOMO-2. (c) Angle dependence of the ionization rate in the plane containing the C–I bond for basis A, B, and C for field strengths of 0.035 au (blue), 0.040 au (green), and 0.045 au (red). (d) Ionization rate (dashed) and contributions from degenerate π HOMO (red), σ HOMO-1 (green), and degenerate π HOMO-2 (blue) in the +X, +Z, and –Z directions as a function of field strength.

X direction is dominated by the HOMO, while both HOMO and HOMO-1 contribute in the Z direction.

The 3D plot for CH₃Br (Figure 5a) shows even more ionization from the halogen p_x orbitals and a small contribution from the methyl group. For CH₃I (Figure 6a), ionization is almost exclusively from the halogen p_x orbitals with almost no contribution from the methyl group. This is in line with the increasing contribution of halogen p_x orbitals to the HOMO (Figures 5b and 6b). The ionization shapes in Figures 5c and 6c clearly show that basis A gives qualitatively incorrect results, while basis B and basis C give similar results. For the X direction, ionization is almost exclusively from the π HOMO, while in the Z directions, both HOMO and HOMO-1 contribute to a similar extent.

SUMMARY

Strong field ionization by intense laser pulses can be simulated with time dependent configuration interaction. A complex absorbing potential needs to be placed around the molecule to model ionization when atom centered basis functions are used.

Standard atom centered basis functions must be augmented by several sets of diffuse functions so that the wave function in the strong laser field can interact with the absorbing potential. The previously developed small absorbing basis is sufficient for CH₃F. Larger absorbing basis sets have been developed for the heavier halogens. A static field was used to probe the angular dependence of ionization of the methyl halides. Ionization of CH₃F occurs mainly from the methyl group. Both the methyl group and the halogen contribute to the strong field ionization of CH₃Cl and CH₃Br. Ionization CH₃I occurs almost exclusively from the p_x orbitals of the iodine.

AUTHOR INFORMATION

Corresponding Author

*E-mail: hbs@chem.wayne.edu; Tel.: 313-577- 2562.

ORCID

H. Bernhard Schlegel: [0000-0001-7114-2821](https://orcid.org/0000-0001-7114-2821)

Notes

The authors declare no competing financial interest.

ACKNOWLEDGMENTS

This work was supported by a grant from National Science Foundation (CHE1464450). We thank the Wayne State University computing grid for the computer time.

REFERENCES

- (1) He, L. H.; Pan, Y.; Yang, Y. J.; Luo, S. Z.; Lu, C. J.; Zhao, H. F.; Li, D. X.; Song, L. L.; Stolte, S.; Ding, D. J.; Roeterdink, W. G. Ion yields of laser aligned CH_3I and CH_3Br from multiple orbitals. *Chem. Phys. Lett.* **2016**, *665*, 141–146.
- (2) Walt, S. G.; Ram, N. B.; von Conta, A.; Tolstikhin, O. I.; Madsen, L. B.; Jensen, F.; Worner, H. J. Role of multi-electron effects in the asymmetry of strong-field ionization and fragmentation of polar molecules: The methyl halide series. *J. Phys. Chem. A* **2015**, *119*, 11772–11782.
- (3) Gitzinger, G.; Loriot, V.; Banares, L.; de Nalda, R. Pulse shaping control of CH_3I multiphoton ionization at 540 nm. *J. Mod. Opt.* **2014**, *61*, 864–871.
- (4) De Nalda, R.; Rubio-Lago, L.; Loriot, V.; Banares, L.; DeNalda, R.; Banares, L. Femtosecond photodissociation dynamics by velocity map imaging. The methyl iodide case. *Springer Ser. Chem. Phys.* **2014**, *107*, 61–97.
- (5) Sun, S. Z.; Yang, Y.; Zhang, J.; Wu, H.; Chen, Y. T.; Zhang, S. A.; Jia, T. Q.; Wang, Z. G.; Sun, Z. R. Ejection of triatomic molecular ion H_3^+ from methyl chloride in an intense femtosecond laser field. *Chem. Phys. Lett.* **2013**, *581*, 16–20.
- (6) Song, Y. D.; Chen, Z.; Sun, C. K.; Hu, Z. Angular distributions of CH_3I fragment ions under the irradiation of a single pulse and trains of ultrashort laser pulses. *Chin. Phys. B* **2013**, *22*, 013302.
- (7) Tang, X. F.; Zhou, X. G.; Wu, M. M.; Liu, S. L.; Liu, F. Y.; Shan, X. B.; Sheng, L. S. Dissociative photoionization of methyl chloride studied with threshold photoelectron-photoion coincidence velocity imaging. *J. Chem. Phys.* **2012**, *136*, 034304.
- (8) Corrales, M. E.; Gitzinger, G.; Gonzalez-Vazquez, J.; Loriot, V.; de Nalda, R.; Banares, L. Velocity map imaging and theoretical study of the Coulomb explosion of CH_3I under intense femtosecond IR pulses. *J. Phys. Chem. A* **2012**, *116*, 2669–2677.
- (9) Yang, Z.; Liu, H. T.; Tang, Z. C.; Gao, Z. Ionization and Dissociation of Methyl Bromide in Intense Laser Field. *Chem. J. Chinese Universities* **2010**, *31*, 367–373.
- (10) Karras, G.; Kosmidis, C. Multielectron dissociative ionization of CH_3I clusters under moderate intensity ps laser irradiation. *Int. J. Mass Spectrom.* **2010**, *290*, 133–141.
- (11) Karras, G.; Kosmidis, C. Angular distribution anisotropy of fragments ejected from methyl iodide clusters: Dependence on fs laser intensity. *Chem. Phys. Lett.* **2010**, *499*, 31–35.
- (12) Wang, Y. M.; Zhang, S.; Wei, Z. R.; Zhang, B. Velocity map imaging of dissociative ionization and coulomb explosion of CH_3I induced by a femtosecond laser. *J. Phys. Chem. A* **2008**, *112*, 3846–3851.
- (13) Tanaka, M.; Murakami, M.; Yatsushashi, T.; Nakashima, N. Atomiclike ionization and fragmentation of a series of $\text{CH}_3\text{-X}$ (X: H, F, Cl, Br, I, and CN) by an intense femtosecond laser. *J. Chem. Phys.* **2007**, *127*, 104314.
- (14) Liu, H. T.; Yang, Z.; Gao, Z.; Tang, Z. C. Ionization and dissociation of CH_3I in intense laser field. *J. Chem. Phys.* **2007**, *126*, 044316.
- (15) Ma, R.; Wu, C. Y.; Xu, N.; Huang, J.; Yang, H.; Gong, Q. H. Geometric alignment of CH_3I in an intense femtosecond laser field. *Chem. Phys. Lett.* **2005**, *415*, 58–63.
- (16) Siozos, P.; Kaziannis, S.; Kosmidis, C. Multielectron dissociative ionization of CH_3I under strong picosecond laser irradiation. *Int. J. Mass Spectrom.* **2003**, *225*, 249–259.
- (17) Graham, P.; Ledingham, K. W. D.; Singhai, R. P.; Hankin, S. M.; McCanny, T.; Fang, X.; Kosmidis, C.; Tzallas, P.; Taday, P. F.; Langley, A. J. On the fragment ion angular distributions arising from the tetrahedral molecule CH_3I . *J. Phys. B: At., Mol. Opt. Phys.* **2001**, *34*, 4015–4026.
- (18) Ford, J. V.; Zhong, Q.; Poth, L.; Castleman, A. W. Femtosecond laser interactions with methyl iodide clusters. I. Coulomb explosion at 795 nm. *J. Chem. Phys.* **1999**, *110*, 6257–6267.
- (19) Ford, J. V.; Poth, L.; Zhong, Q.; Castleman, A. W. Femtosecond laser interactions with methyl iodide clusters. 2. Coulomb explosion at 397 nm. *Int. J. Mass Spectrom.* **1999**, *192*, 327–345.
- (20) Trinh, V. H.; Pham, V. N. T.; Tolstikhin, O. I.; Morishita, T. Weak-field asymptotic theory of tunneling ionization including the first-order correction terms: Application to molecules. *Phys. Rev. A: At., Mol., Opt. Phys.* **2015**, *91*, 063410.
- (21) Tolstikhin, O. I.; Madsen, L. B.; Morishita, T. Weak-field asymptotic theory of tunneling ionization in many-electron atomic and molecular systems. *Phys. Rev. A: At., Mol., Opt. Phys.* **2014**, *89*, 013421.
- (22) Trinh, V. H.; Tolstikhin, O. I.; Madsen, L. B.; Morishita, T. First-order correction terms in the weak-field asymptotic theory of tunneling ionization. *Phys. Rev. A: At., Mol., Opt. Phys.* **2013**, *87*, 043426.
- (23) Madsen, L. B.; Tolstikhin, O. I.; Morishita, T. Application of the weak-field asymptotic theory to the analysis of tunneling ionization of linear molecules. *Phys. Rev. A: At., Mol., Opt. Phys.* **2012**, *85*, 053404.
- (24) Krause, P.; Schlegel, H. B. Strong-field ionization rates of linear polyenes simulated with time-dependent configuration interaction with an absorbing potential. *J. Chem. Phys.* **2014**, *141*, 174104.
- (25) Krause, P.; Sonk, J. A.; Schlegel, H. B. Strong field ionization rates simulated with time-dependent configuration interaction and an absorbing potential. *J. Chem. Phys.* **2014**, *140*, 174113.
- (26) Krause, P.; Schlegel, H. B. Angle-dependent ionization of hydrides AH_n calculated by time-dependent configuration interaction with an absorbing potential. *J. Phys. Chem. A* **2015**, *119*, 10212–10220.
- (27) Krause, P.; Schlegel, H. B. Angle-dependent ionization of small molecules by time-dependent configuration interaction and an absorbing potential. *J. Phys. Chem. Lett.* **2015**, *6*, 2140–2146.
- (28) Liao, Q.; Li, W.; Schlegel, H. B. Angle-dependent strong-field ionization of triple bonded systems calculated by time-dependent configuration interaction with an absorbing potential. *Can. J. Chem.* **2016**, *94*, 989–997.
- (29) Hoerner, P.; Schlegel, H. B. Angular dependence of ionization by circularly polarized light calculated with time-dependent configuration interaction with an absorbing potential. *J. Phys. Chem. A* **2017**, *121*, 1336–1343.
- (30) Sissay, A.; Abanador, P.; Mauger, F.; Gaarde, M.; Schafer, K. J.; Lopata, K. Angle-dependent strong-field molecular ionization rates with tuned range-separated time-dependent density functional theory. *J. Chem. Phys.* **2016**, *145*, 094105.
- (31) Frisch, M. J.; Trucks, G. W.; Schlegel, H. B.; Scuseria, G. E.; et al. *Gaussian Development Version*, revision I.09; Gaussian, Inc.: Wallingford, CT, 2010.
- (32) Dunning, T. H. Gaussian-basis sets for use in correlated molecular calculations 0.1. The atoms boron through neon and hydrogen. *J. Chem. Phys.* **1989**, *90*, 1007–1023.
- (33) Woon, D. E.; Dunning, T. H., Jr. Gaussian basis sets for use in correlated molecular calculations. III. The atoms aluminum through argon. *J. Chem. Phys.* **1993**, *98*, 1358–1371.
- (34) Peterson, K. A.; Shepler, B. C.; Figgen, D.; Stoll, H. On the spectroscopic and thermochemical properties of ClO, BrO, IO, and their anions. *J. Phys. Chem. A* **2006**, *110*, 13877–13883.